Supplemental material: Control of electron wave packets close to the continuum threshold using near-single-cycle THz waveforms

Simon Brennecke,[1] Martin Ranke,[2,3] Anastasios Dimitriou,[2,3,4] Sophie Walther,[2,3] Mark J. Prandolini,[2] Manfred Lein,[1] and Ulrike Frühling[2,3,5]

[1] *Leibniz Universität Hannover, Institut für Theoretische Physik, Appelstraße 2, 30167 Hannover, Germany*
[2] *Institut für Experimentalphysik, Universität Hamburg, Luruper Chaussee 149, 22761 Hamburg, Germany*
[3] *The Hamburg Centre for Ultrafast Imaging (CUI), Luruper Chaussee 149, 22761 Hamburg, Germany*
[4] *Institute of Nanoscience and Nanotechnology, NSR Demokritos, Aghia Paraskevi, Athens, Greece*
[5] *Deutsches Elektronen-Synchrotron, Notkestrasse 85, 22603 Hamburg, Germany*

(Dated: September 10, 2022)

CLASSICAL TRAJECTORY SIMULATIONS

The trajectory simulations presented in the main text allow us to give a classical interpretation of the electron dynamics. In addition, the framework enables us to study the influence of a weak, but long tail of the THz pulse as well as the influence of the static detector field of the velocity-map imaging spectrometer (VMI). To this end, we perform additional classical calculations where we restrict ourselves to the 2D dynamics in the plane spanned by the polarization axis (x-axis) and the detector field pointing in negative y-direction.

The photoelectron momentum distributions along the polarization axis are shown in Fig. S1(a) for the short THz pulse of only 2.9 ps duration, see Fig. S2. Even though this delay trace contains all prominent features of the 3D calculations shown in Fig. 2(c) of the main text, their relative intensities are slightly changed due to the reduced dimensionality. In order to study the effect of a more realistic THz pulse with an extended tail, we perform simulations for a long pulse with a tail of $\approx$ 15 kV/cm maximal field strength at $t \approx 1.4$ ps and reaching zero at $t = 10$ ps, see Fig. S2. Our conclusions do not depend on the precise length of the THz pulse tail. All prominent structures in the low-energy region with $|p_x| > 0.04$ a.u. are basically unchanged (see Fig. S1(c)) compared to the result for a short pulse. As expected, slightly more electrons with very low kinetic energies ($|p_x| < 0.04$ a.u.) are set free by the pulse tail. However, we find that even the inclusion of a pulse tail cannot fully reproduce the strong signal of zero-energy electrons visible in the experiment.

For these zero-energy electrons, the detector field of the VMI plays a crucial role [1, 2]. The static field may induce an additional collision of continuum electrons with very low energies and, thus, may modify their dynamics. This interplay between the detector field and the long-range electron-ion interaction can lead to deviations from parabolic trajectories usually assumed to interpret VMI measurements [3]. The detector field also leads to additional ionization of Rydberg states [4, 5].

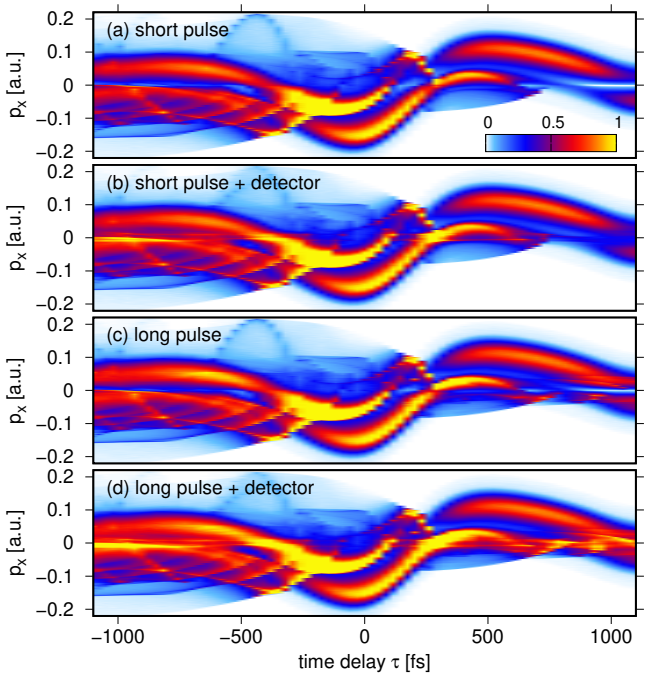

FIG. S1. Electron momentum distribution along the polarization direction (p_x-direction) from classical simulations in 2D versus time delay between the THz waveform and the NIR pulse. The distributions are obtained by integration of the momentum distribution over the p_y-component. Panels (a)-(d) show results for the four possible settings based on either a short or a long THz pulse and the detector field being included or neglected.

The inclusion of the detector field in the classical simulations results in the p_x-distributions shown in Figs. S1(b) and (d) for the short and long THz pulses, respectively. Even though the dynamics is modified strongly in the direction of the detector field, the numerical calculations confirm that in the projected momentum distributions (detector images) only zero-energy electrons ($|p_x| < 0.04$ a.u.) are non-trivially influenced by the detector field. In contrast, for low-energy electrons with $|p_x| > 0.04$ a.u. all structures are still present and their

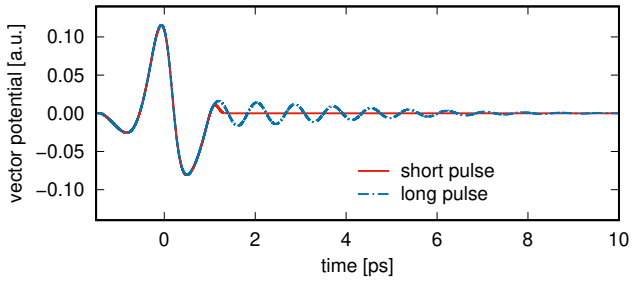

FIG. S2. Vector potentials of the THz fields used in the classical simulations.

intensities are only very weakly changed so that a non-trivial influence of the detector field can be neglected. Our findings are in agreement with the previous theoretical study by Bordas [1] where it has been shown that the characteristic energy scale in the Stark problem is given by $E_c = 2\sqrt{ZF}$. We have $E_c = 4 \times 10^{-4}$ a.u. for a detector field strength $F = 4 \times 10^{-8}$ a.u. and an asymptotic charge $Z = 1$ a.u. Thus, the corresponding momentum scale is given by $p_c = \sqrt{2E_c} \approx 0.028$ a.u.

Considering a THz pulse with tail and including the detector field results in a strong additional signal of zero-energy electrons (in agreement with the experimental data). Since we are unable to resolve experimentally the fine structures visible in the simulations, we only discuss further the integrated yield of zero-energy electrons. In Fig. S3(b), the integrated probability is shown for the four settings discussed above. For delays around $\tau = 0$ fs, the main part of the THz pulse already ionizes efficiently all weakly-bound electrons and, hence, neither the tail nor the detector field lead to additional ionization. Thus, all settings give approximately the same zero-energy yield. In contrast, for large positive and negative delays, both the pulse tail as well as the detector field give rise to additional zero-energy electrons. In the presence of the pulse tail, the electrons may pick up some additional energy. Even though only a fraction is ionized by the pulse tail itself, the additional excitation leads to more electrons that are freed by the detector field compared to the short pulse case.

For a simplified modeling, we can split the process in two parts: (i) The THz pulse dominates the dynamics as long as it is present and the detector field can be neglected. (ii) After the end of the THz pulse, there is still population left in very weakly bound states that is afterwards freed by the detector field. In Ref. [6], it has been shown for a simplified velocity distribution that the static field ionizes two-thirds of the electrons with energies $-E_c < E < 0$. For the 2D system, we find that this simple estimate (black thick line) reproduces very well the result of a full classical calculation including both the long pulse as well as detector field (blue dotted line). Hence, we use the analogous procedure to estimate

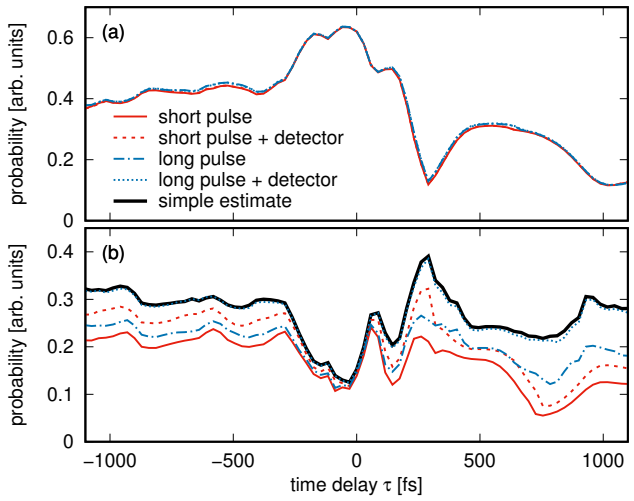

FIG. S3. Integrated probabilities versus time delay obtained from 2D classical simulations. (a) Probability of low-energy electrons except for zero-energy electrons, obtained by integration over all momenta satisfying $|p_x| > 0.04$ a.u. (b) Probability of zero-energy electrons ($|p_x| < 0.04$ a.u.). The four settings indicated in the legend are the same as in Fig. S1. In addition, the black thick line shows the sum of the classical model for a long THz pulse and the estimated amount of Rydberg-state population freed by the detector field.

the amount of zero-energy electrons freed by the detector field in 3D. These 3D results are shown in Fig. 4(b) of the main text.

[1] C. Bordas, "Classical motion of a photoelectron interacting with its ionic core: Slow photoelectron imaging," Phys. Rev. A **58**, 400 (1998).

[2] C. Nicole, I. Sluimer, F. Rosca-Pruna, M. Warntjes, M. Vrakking, C. Bordas, F. Texier, and F. Robicheaux, "Slow photoelectron imaging," Phys. Rev. Lett. **85**, 4024 (2000).

[3] A. T. J. B. Eppink and D. H. Parker, "Velocity map imaging of ions and electrons using electrostatic lenses: Application in photoelectron and photofragment ion imaging of molecular oxygen," Rev. Sci. Instrum. **68**, 3477 (1997).

[4] J. Dura, N. Camus, A. Thai, A. Britz, M. Hemmer, M. Baudisch, A. Senftleben, C. D. Schröter, J. Ullrich, R. Moshammer, and J. Biegert, "Ionization with low-frequency fields in the tunneling regime," Sci. Rep. **3**, 2675 (2013).

[5] B. Wolter, C. Lemell, M. Baudisch, M. G. Pullen, X.-M. Tong, M. Hemmer, A. Senftleben, C. D. Schröter, J. Ullrich, R. Moshammer, J. Biegert, and J. Burgdörfer, "Formation of very-low-energy states crossing the ionization threshold of argon atoms in strong mid-infrared fields," Phys. Rev. A **90**, 063424 (2014).

[6] E. Diesen, U. Saalmann, M. Richter, M. Kunitski, R. Dörner, and J. M. Rost, "Dynamical characteristics of Rydberg electrons released by a weak electric field," Phys. Rev. Lett. **116**, 143006 (2016).